Imaging shapes of atomic nuclei in high-energy nuclear collisions from STAR experiment

Chunjian Zhang

(for the STAR Collaboration)

INPC 2025, May 25-30, 2025, Daejeon, Korea

STAR 25 YEARS

INPC 2025

Supported by the U.S. DEPARTMENT OF ENERGY

Nuclear shape at low energy: long exposure

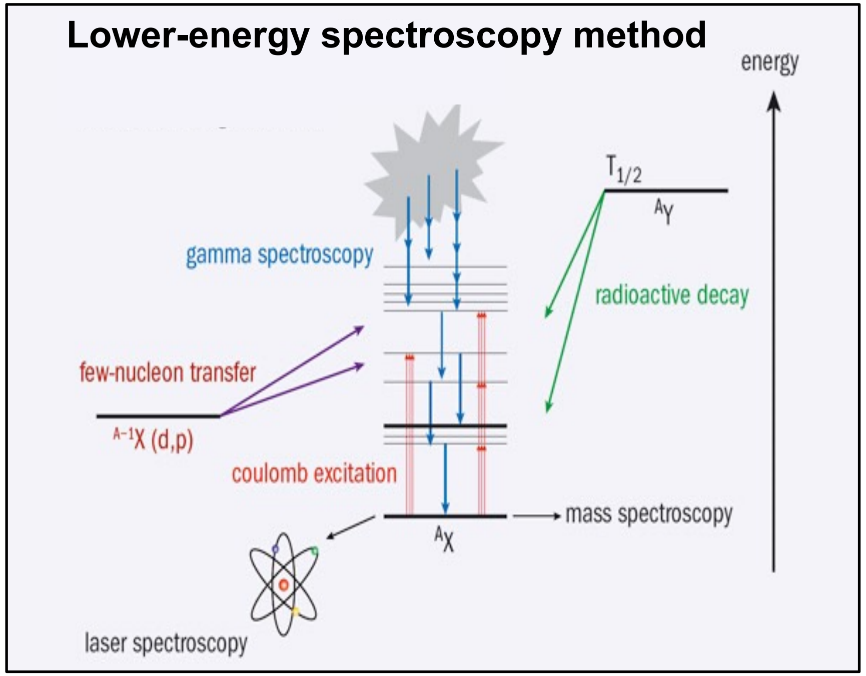

Emergent phenomena of the many-body quantum system

- Quadrupole/octupole/hexadecapole deformations
- Clustering, halo, skin, bubble…
- Non-monotonic evolution with *N* and Z

Traditional imaging method taken before destruction

→ Low energy spectroscopic methods probe a superposition of these fluctuations.

→ Instantaneous shapes not directly seen, but inferred from model comparison.

Each DOF has zero-point fluctuations within certain timescales.

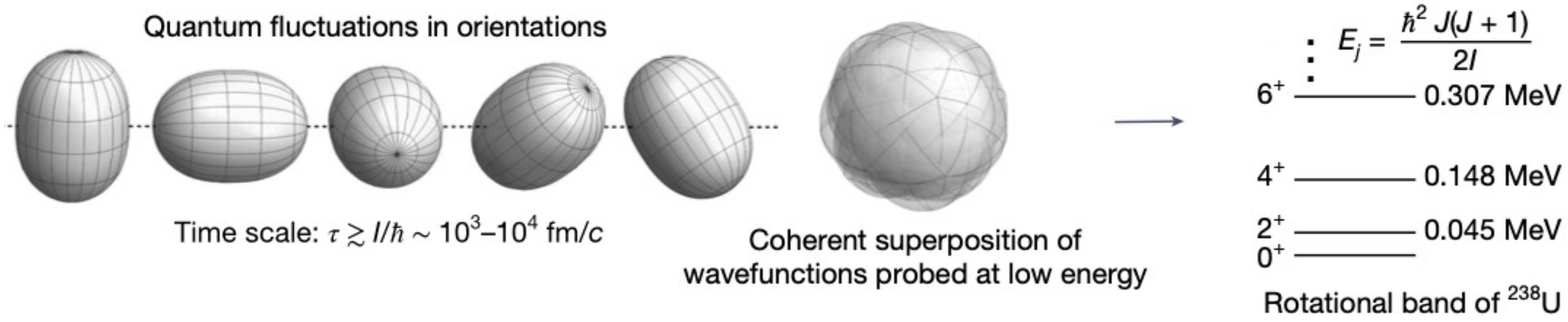

Nuclear shape at high-energy: short exposure

Emergent seeing shape directly require access to instantaneous nucleon distributions

$$\Psi(\mathbf{r}_1, \mathbf{r}_2 \ldots)$$

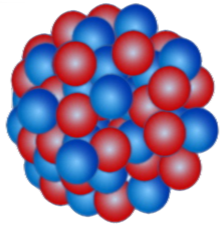

Will see all DOFs longer than exposure timescale: $\tau > \tau_{\mathrm{expo}}$

nucleons, hadrons, quark, gluons, gluon saturations

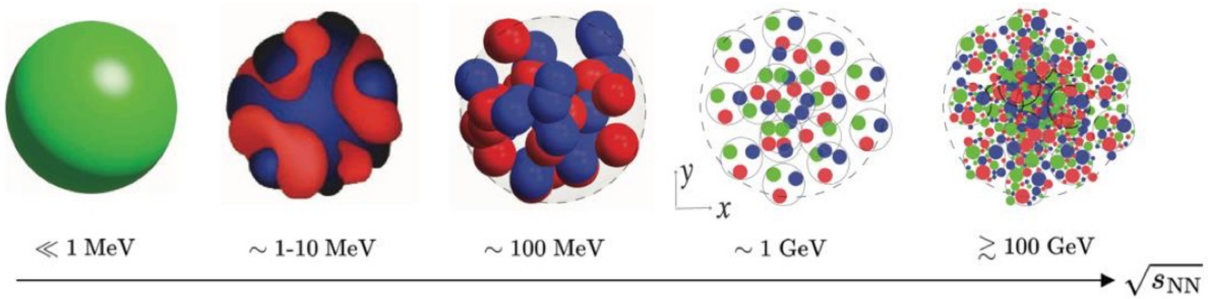

Hence concept of shape is collision energy dependent

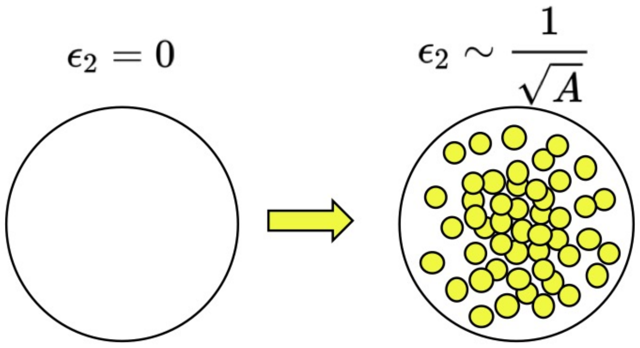

Spherical Woods-saxon

Sampled with A nucleons

$$\boldsymbol{\epsilon}_2 = \underbrace{\boldsymbol{\epsilon}_0} + \underbrace{\boldsymbol{p}(\Omega)\beta_2} + \mathcal{O}\left(\beta_2^2\right)$$

$\sqrt{s}$-dependent quantum fluctuation induced shape

Global shape rotational vibrational

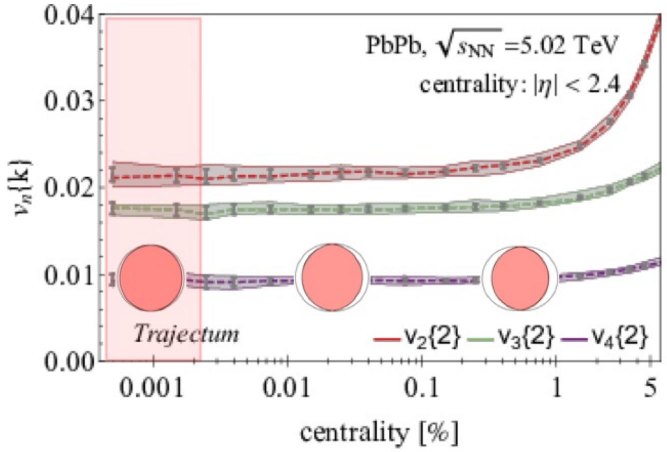

Imaging by smashing method

Take a snapshot | Evolution | Measurement

Nuclei collisions

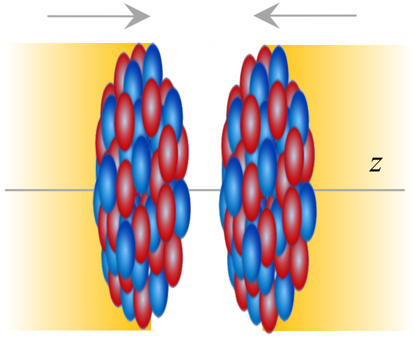

$T_{\mu\nu}(\tau = 0)$

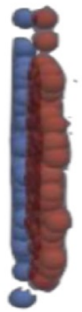

$\tau \sim 2R_0/\Gamma \sim 0.1\mathrm{fm}/c$
exposure

$\partial_\mu T^{\mu\nu} = 0$, EOS, viscosity…

Pressure-driven expansion of Quark-gluon plasma (QGP)

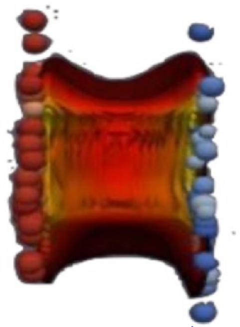

$\tau \sim 10\mathrm{fm}/c$
expansion

free-streaming

$T_{\mu\nu}(\tau = \infty)$

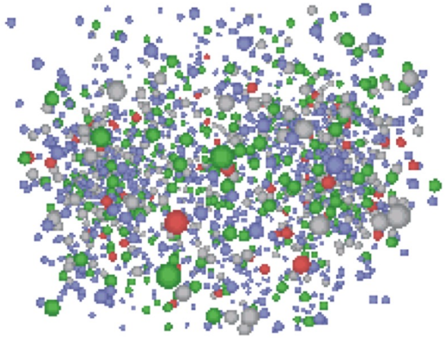

$\tau \sim 10^{15}\mathrm{fm}/c$
detection

$T_{\mu\nu}(\tau = 0)$ snapshot ⟶ $\partial_\mu T^{\mu\nu} = 0$ evolution ⟶ $T_{\mu\nu}(\tau = \infty)$ measurement

J. Jia et al., Nucl. Sci. Tech 35, 220 (2024)

Image inferred after destruction

Imaging by smashing method

Take a snapshot — Evolution — Measurement

Nuclei collisions

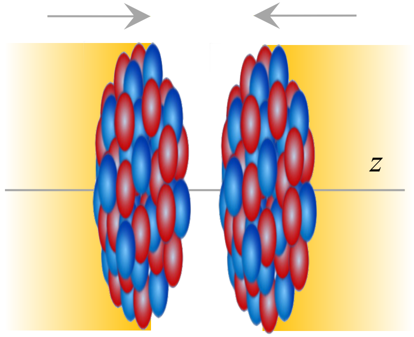

$T_{\mu\nu}(\tau = 0)$

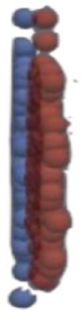

$\tau \sim 2R_0/\Gamma \sim 0.1\mathrm{fm}/c$
exposure

Pressure-driven expansion of Quark-gluon plasma (QGP)

$\partial_\mu T^{\mu\nu} = 0$, EOS, viscosity…

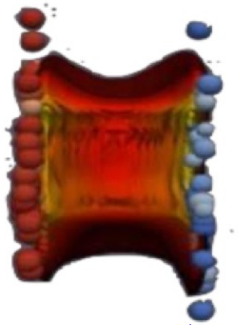

$\tau \sim 10\mathrm{fm}/c$
expansion

free-streaming

$T_{\mu\nu}(\tau = \infty)$

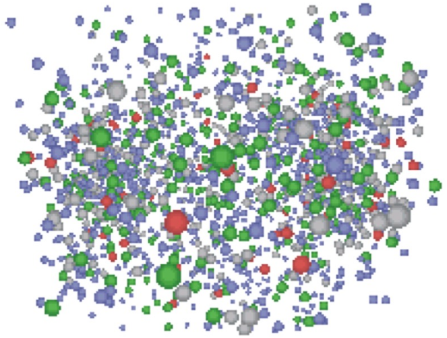

$\tau \sim 10^{15}\mathrm{fm}/c$
detection

Large entropy production enable a semi-classical description

- Initial condition is a fast snapshot of nuclear structure (<0.1fm/c)
- Transformed to the final state via hydrodynamic expansion
- Reverse-engineer to infer the snapshot, aided by large information output

J. Jia et al., Nucl. Sci. Tech 35, 220 (2024)

Ability to image ⟷ Understanding of the QGP

Imaging by smashing method

Take a snapshot

Nuclei collisions

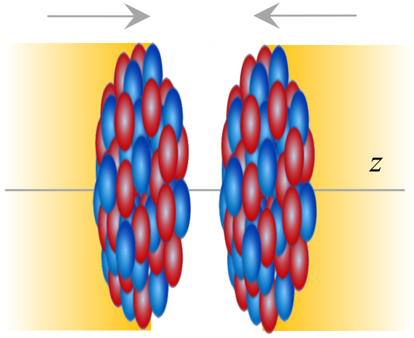

$T_{\mu\nu}(\tau=0)$

$\tau \sim 2R_0/\Gamma \sim 0.1\mathrm{fm}/c$

exposure

$$\rho(r,\theta,\phi)=\frac{\rho_0}{1+e^{(r-R(\theta,\phi))/a_0}}$$

- β_2 → quadrupole deformation
- β_3 → octupole deformation
- γ → triaxiality
- a_0 → surface diffuseness
- R_0 → nuclear size

ab initio theory/shell model/DFT

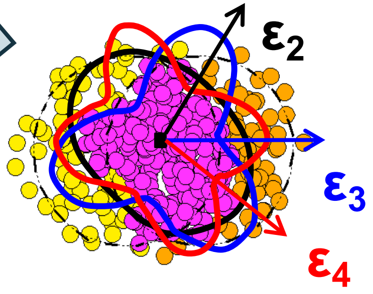

size & shape

Evolution

$\partial_\mu T^{\mu\nu}=0$, EOS, viscosity…

Pressure-driven expansion of

Quark-gluon plasma (QGP)

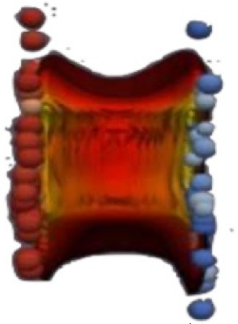

$\tau \sim 10\mathrm{fm}/c$

expansion

$R_\perp^2 \propto \langle r_\perp^2 \rangle$ $\quad$ $\mathcal{E}_n \propto \langle r_\perp^n e^{in\phi} \rangle$

R_0 $\quad$ a_0 $\quad$ β_n

Measurement

free-streaming

$T_{\mu\nu}(\tau=\infty)$

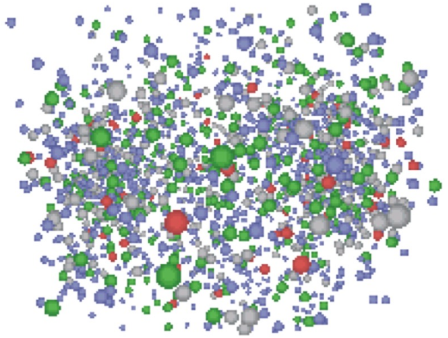

$\tau \sim 10^{15}\mathrm{fm}/c$

detection

observables

$$\frac{d^2N}{d\phi dp_T}=N(p_T)\left(\sum_n V_n e^{-in\phi}\right)$$

Event-by-event linear responses:

$$\frac{\delta[p_T]}{[p_T]} \propto -\frac{\delta R_\perp}{R_\perp} \qquad V_n \propto \mathcal{E}_n$$

Key: 1) fast snapshot (yoctoseconds), 2) linear response, 3) large multiplicity for many-body correlation

STAR detector at BNL

Time Projection Chamber

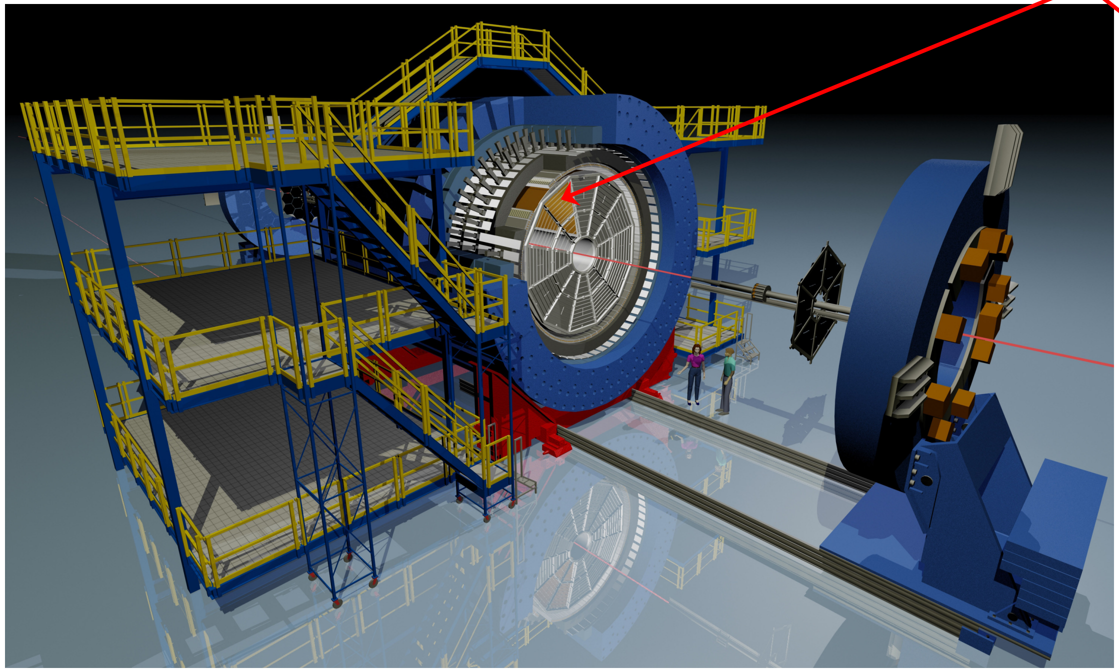

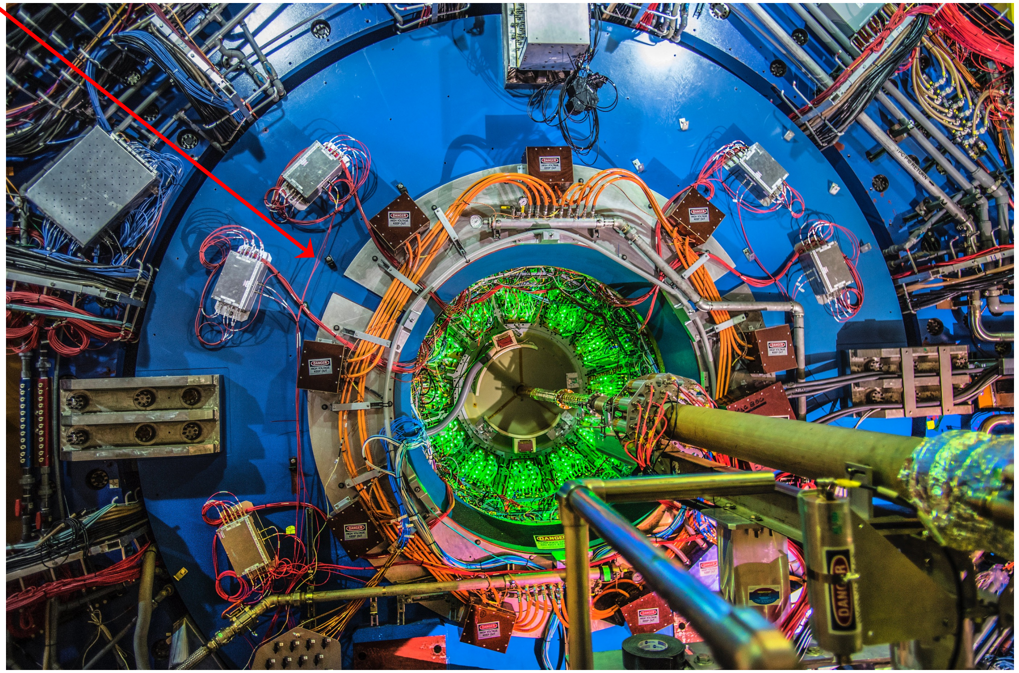

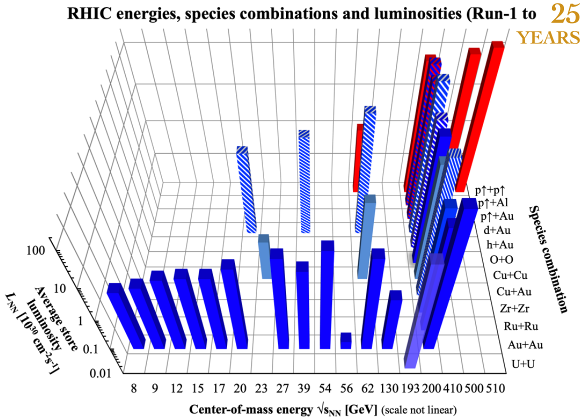

STAR detector provides

1) Large/uniform acceptance, better centrality resolution

2) Sufficient statistics for emitted final-state hadrons

3) Different collision systems: U+U, Au+Au, Ru+Ru, Zr+Zr, O+O …

Nuclear structure in heavy ^{238}U nucleus

$$\rho(r,\theta,\phi) = \frac{\rho_0}{1+e^{(r-R(\theta,\phi))/a_0}}$$

$$R(\theta,\phi) = R_0\left(1+\beta_2\left[\cos\gamma Y_{2,0}(\theta,\phi)+\sin\gamma Y_{2,2}(\theta,\phi)\right]+\beta_3 Y_{3,0}(\theta,\phi)+\beta_4 Y_{4,0}(\theta,\phi)\right)$$

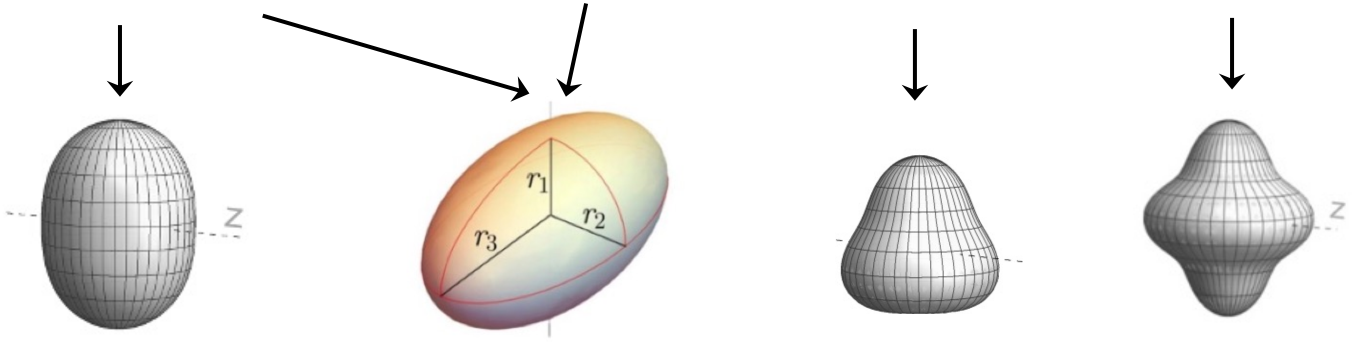

Imaging nuclear shape in high-energy snapshot as a novel way

- Nuclear shape in intrinsic (body-fixed) frame not directly visible in the lab frame
  --Mainly inferred from non-invasive spectroscopy methods.

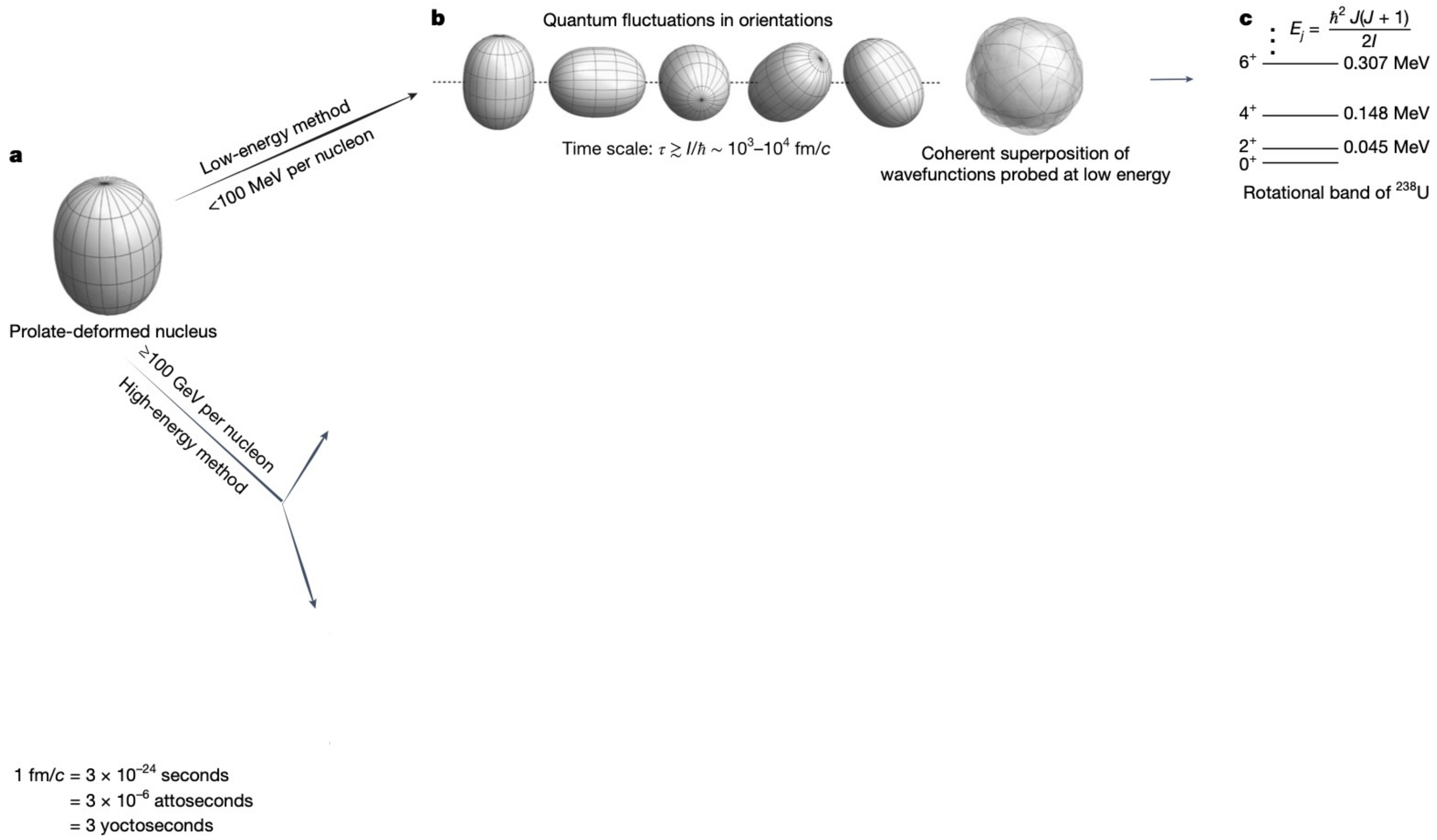

Imaging nuclear shape in high-energy snapshot as a novel way

- Nuclear shape in intrinsic (body-fixed) frame not directly visible in the lab frame

  --Mainly inferred from non-invasive spectroscopy methods.

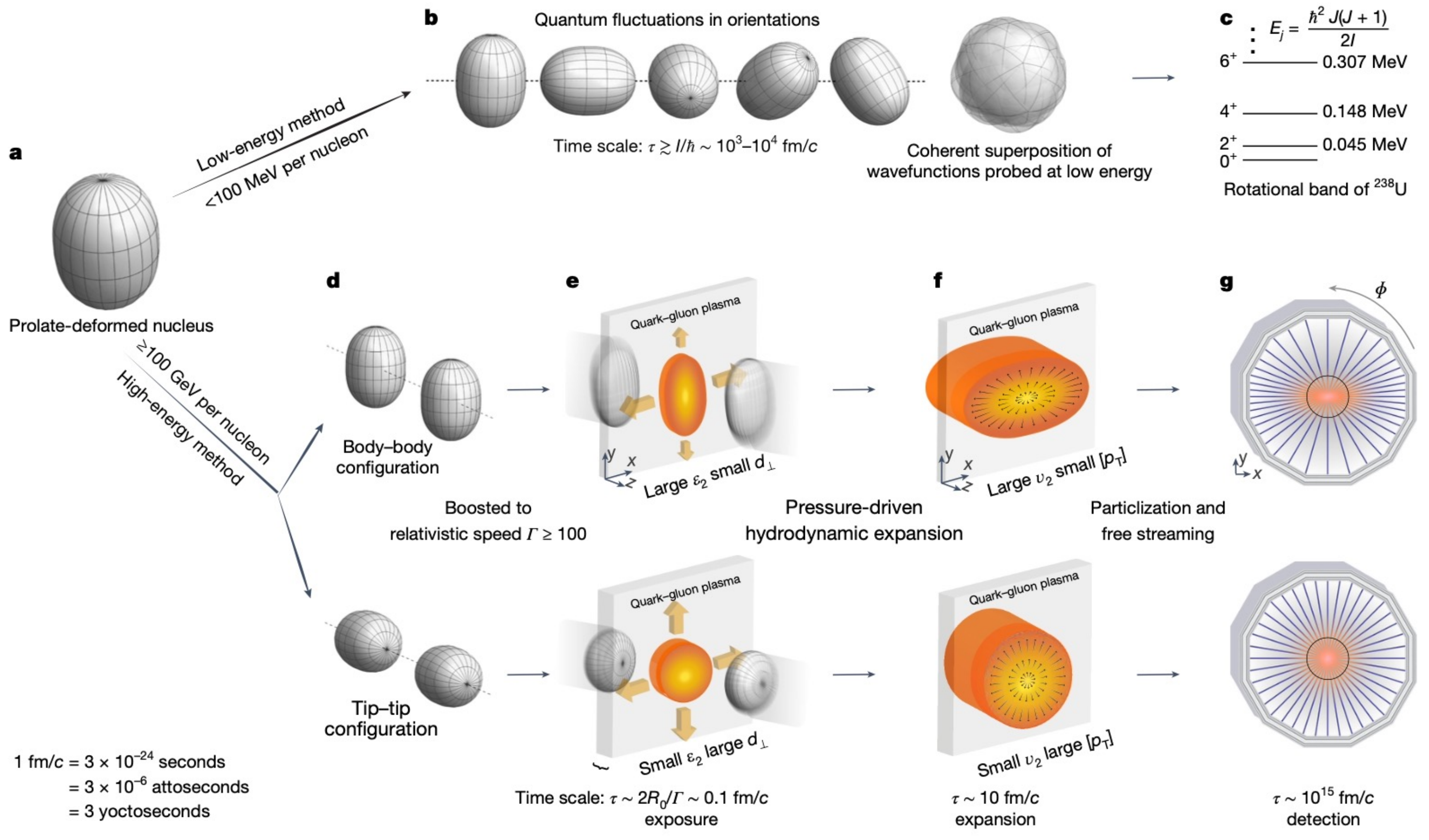

STAR, Nature 635, 67-72 (2024)

https://www.nature.com/articles/s41586-024-08097-2

across energy scales

Body-body: large-eccentricity large-size

$v_2 \nearrow$ $p_T \searrow$

Tip-tip : small-eccentricity small-size

$v_2 \searrow$ $p_T \nearrow$

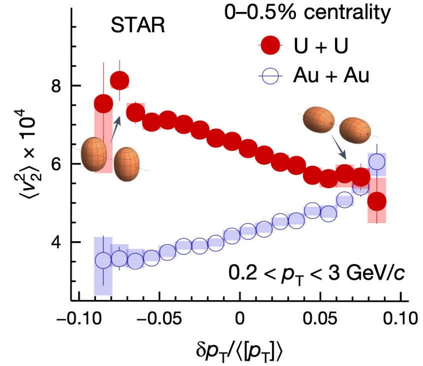

Shape-frozen like a snapshot during nuclear crossing (10^{-25}s << rotational time scale 10^{-21}s)

probe entire mass distribution in the intrinsic frame via multi-point correlations

Ratio of observables

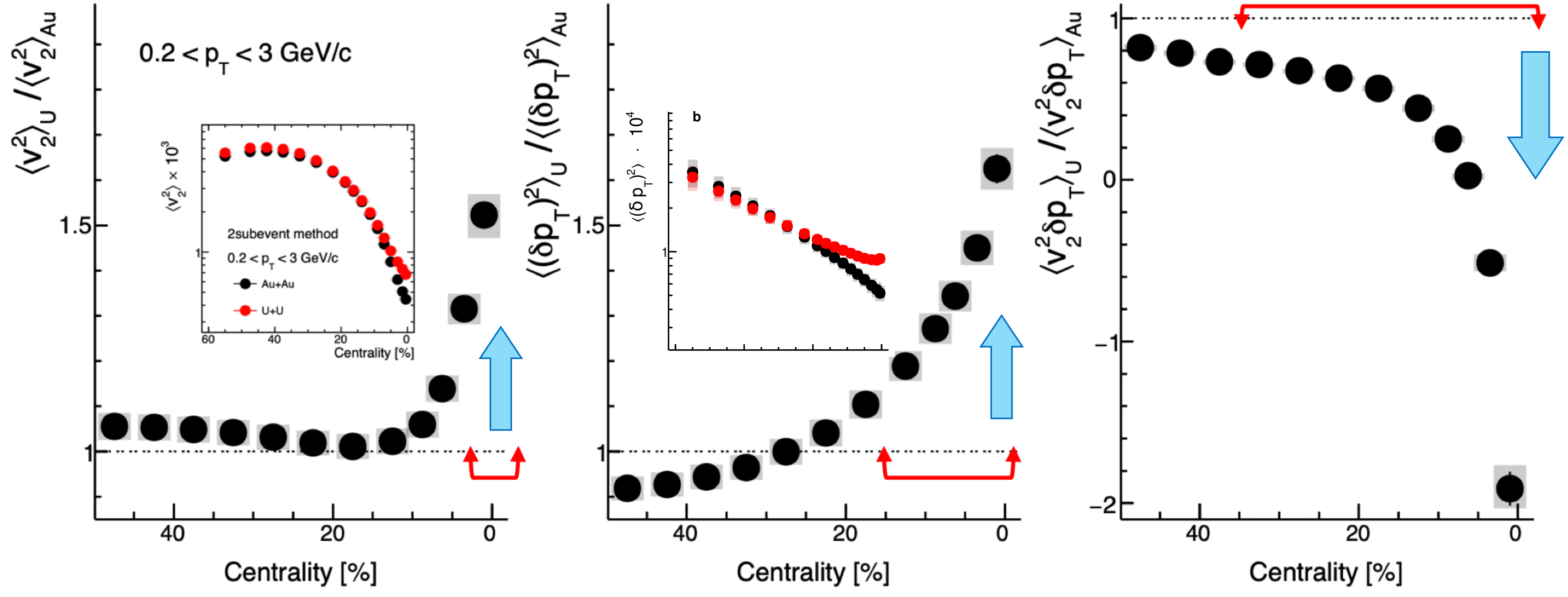

$$R_{\langle v_2^2\rangle} \approx 1 + \frac{b_1}{a_1}\beta_2^2,$$
$$R_{\langle (\delta p_T)^2\rangle} \approx 1 + \frac{b_2}{a_2}\beta_2^2,$$
$$R_{\langle v_2^2 \delta p_T\rangle} \approx 1 - \frac{b_3}{a_3}\beta_2^3\cos(3\gamma)$$

- Elliptic flow and size fluctuation are enhanced by the nuclear deformation effect.
- Ratios cancel final state effects and isolate the effects of initial state/nuclear structures.

→ U deformation dominates the ultra-central collisions (UCC)

G. Giacalone, J. Jia, C. Zhang, PRL 127, 242301(2021)

Imaging shape of the ground-state ^{238}U: β_2 and γ

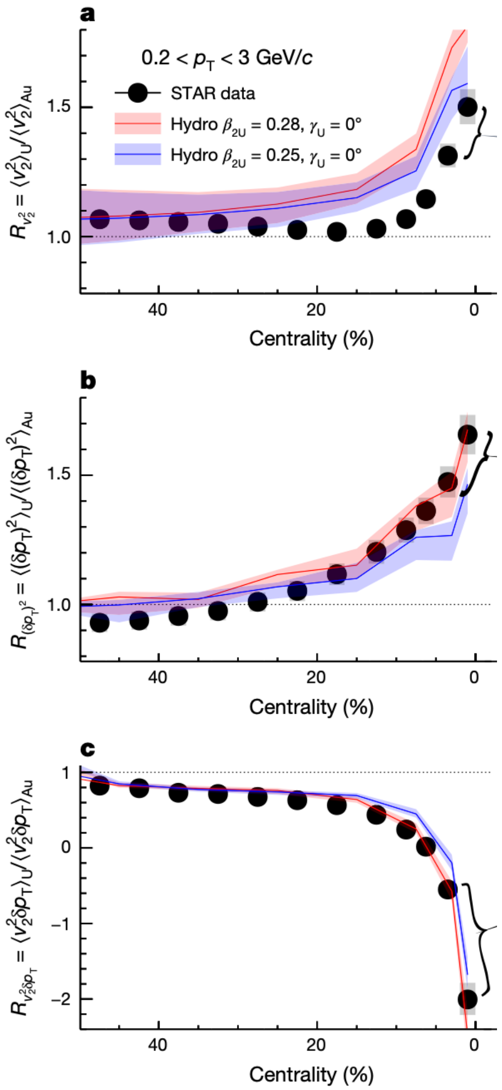

Imaging shape of the ground-state ^{238}U: β_2 and γ

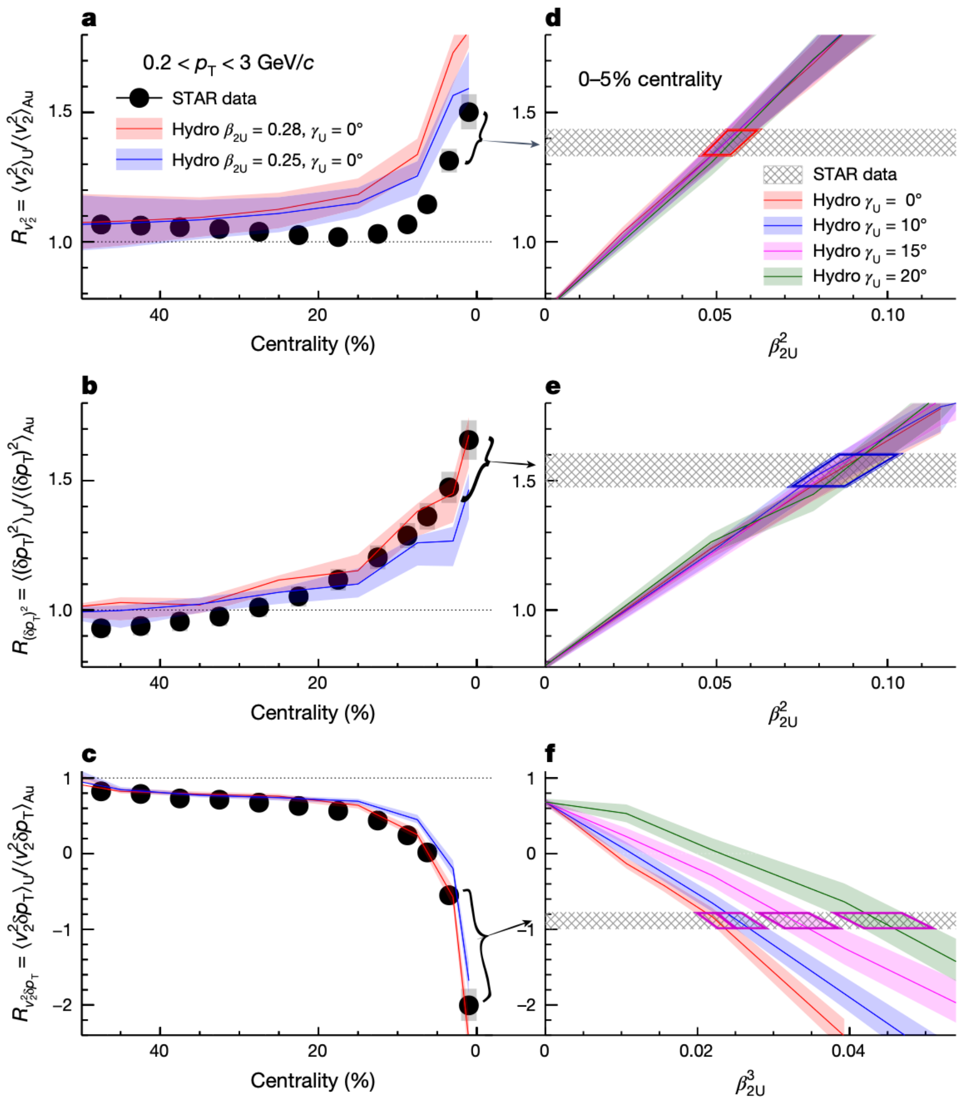

Sufficient precision is achieved from ratios in ultra-central collisions

Relation confirmed from hydro

$$\langle v_2^2 \rangle = a_1 + b_1 \beta_2^2$$
$$\left\langle (\delta p_\mathrm{T})^2 \right\rangle = a_2 + b_2 \beta_2^2$$
$$\langle v_2^2 \delta p_\mathrm{T} \rangle = a_3 - b_3 \beta_2^3 \cos(3\gamma)$$

Imaging shape of the ground-state ^{238}U: β_2 and γ

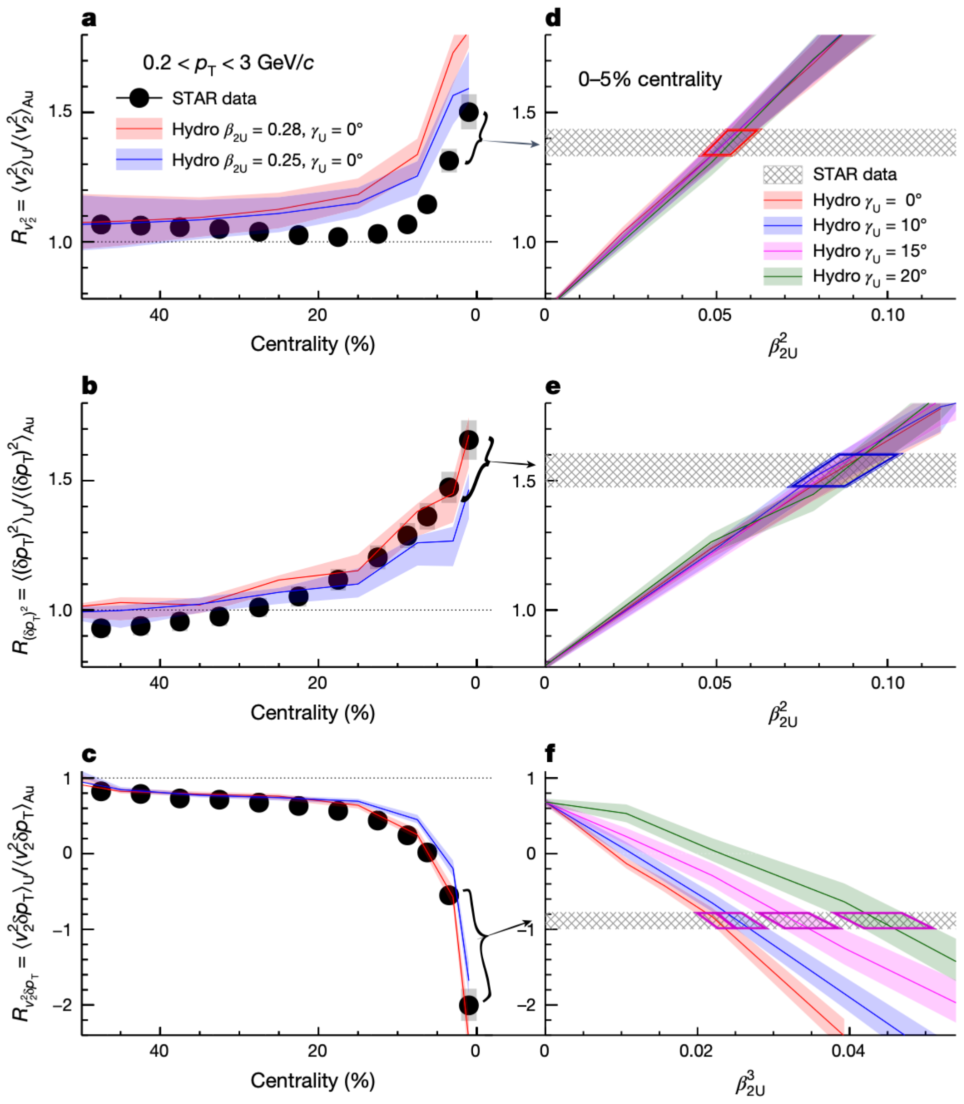

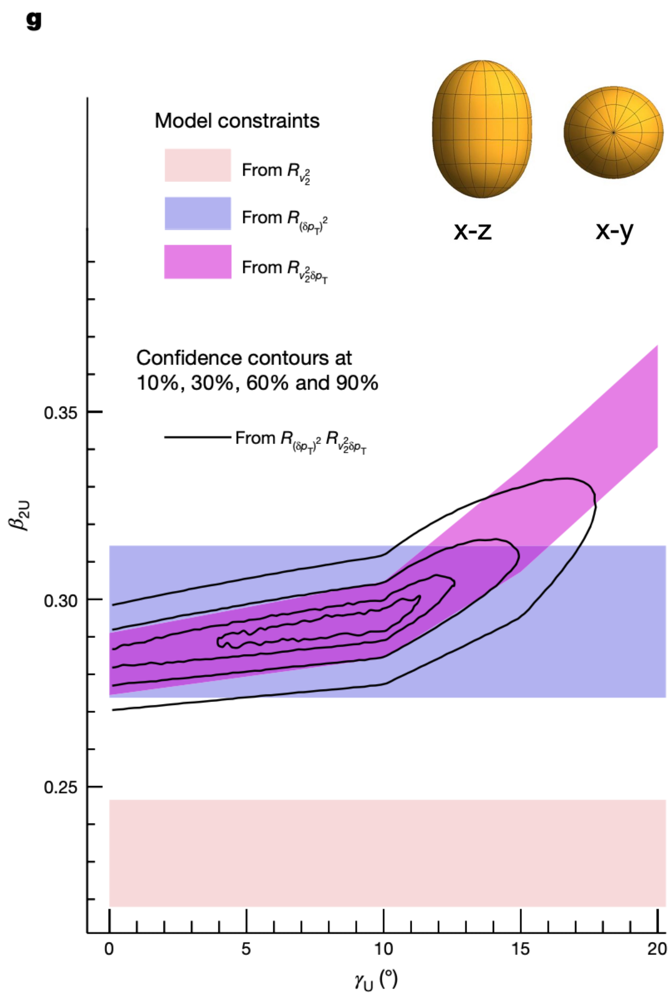

Sufficient precision is achieved from ratios in ultra-central collisions

Relation confirmed from hydro

$$\langle v_2^2 \rangle = a_1 + b_1 \beta_2^2$$
$$\left\langle (\delta p_T)^2 \right\rangle = a_2 + b_2 \beta_2^2$$
$$\langle v_2^2 \delta p_T \rangle = a_3 - b_3 \beta_2^3 \cos(3\gamma)$$

High-energy estimate:

$$\beta_{2U} = 0.286 \pm 0.025$$
$$\gamma_U = 8.5^\circ \pm 4.8^\circ$$

Low-energy estimate:

$$\beta_{2U} = 0.287 \pm 0.007$$
$$\gamma_U = 6^\circ - 8^\circ$$

A large deformation with a slight deviation from axial symmetry in the nuclear ground-state

Probing octupole deformation in ^{238}U

SATR measurement

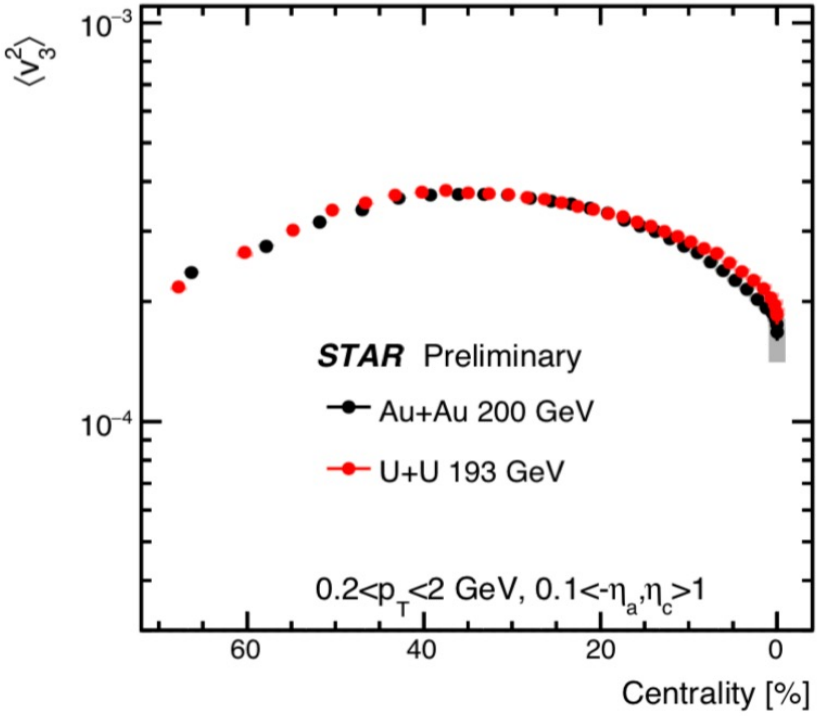

model prediction

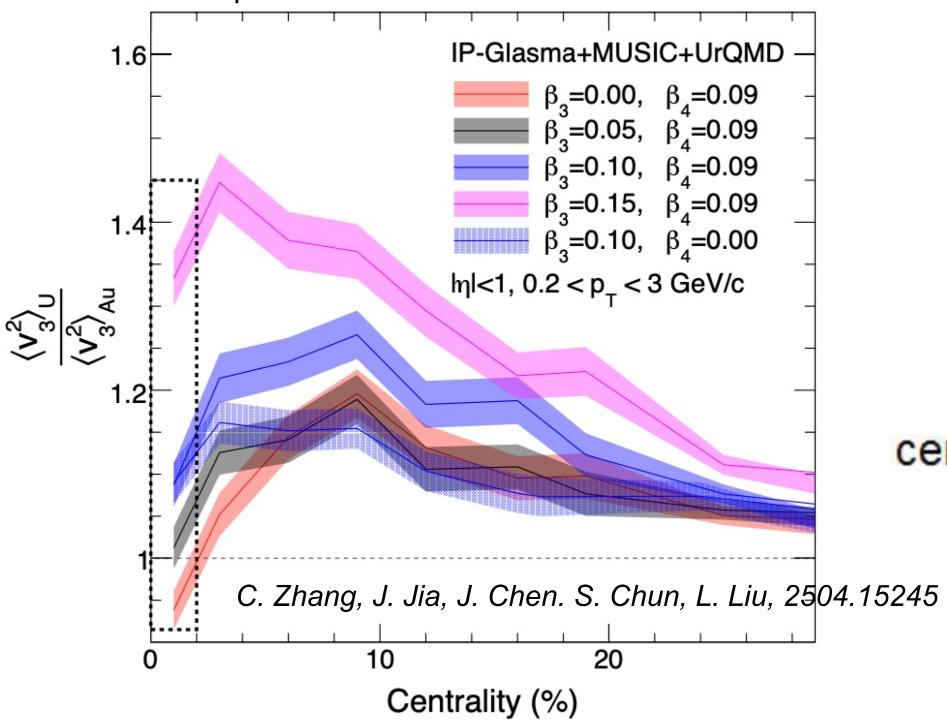

Octupole deformation enhanced atomic EDM moment

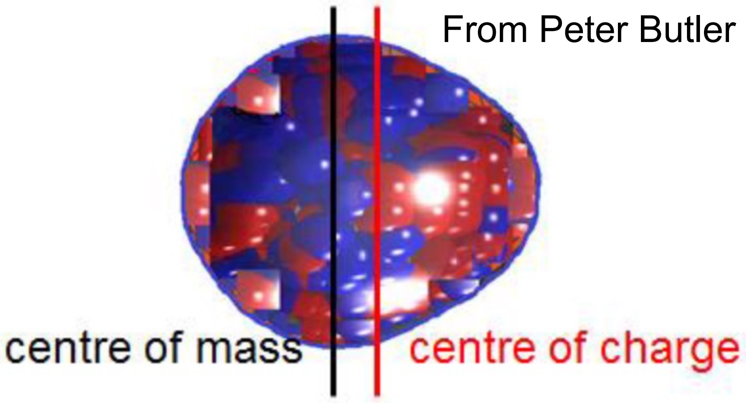

v_3 is fluctuation driven, expect in central

$$\langle v_3^2 \rangle \propto \langle \varepsilon_3^2 \rangle \sim 1/A$$

mass number

finite size and shape of nucleus breaks the symmetry

Higher sensitivity via Schiff nuclear moments in heavy nuclei

rigid per-shape or octupole vibration?

Nature 497, 199 (2013); Rev. Mod. Phys. 91, 015001 (2019); Rep. Prog. Phys. 80, 046301 (2017); Ann. Rev. Nucl. Part. Sci. 69, 219 (2019); The 2023 Long-rang plan for nuclear physics

STAR manuscript is in preparation.

Nuclear structure in isobaric ^{96}Ru and ^{96}Zr nuclei

$$\rho(r,\theta,\phi) = \frac{\rho_0}{1+e^{(r-R(\theta,\phi))/a_0}} \longrightarrow$$

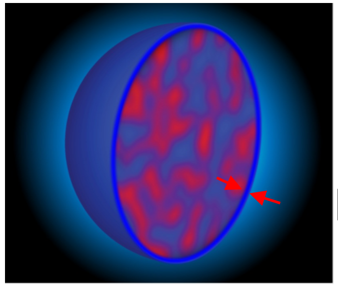

R_n-R_p

$$R(\theta,\phi) = R_0\left(1+\beta_2\left[\cos\gamma Y_{2,0}(\theta,\phi)+\sin\gamma Y_{2,2}(\theta,\phi)\right]+\beta_3 Y_{3,0}(\theta,\phi)+\beta_4 Y_{4,0}(\theta,\phi)\right)$$

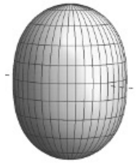

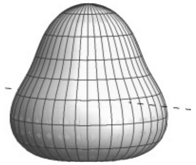

large $\beta_{2,\mathrm{Ru}}$, larger $\beta_{3,\mathrm{Zr}}$ with large uncertainties.

	β_2	$E_{2_1^+}$ (MeV)	β_3	$E_{3_1^-}$ (MeV)
^{96}Ru	0.154	0.83	-	3.08
^{96}Zr	0.062	1.75	0.202,0.235,0.27	1.90

Evidence of static octupole moments at low energies is rather sparse.

Nuclear structure via collectivity v_n ratio $\frac{\mathcal{O}_{^{96}\mathrm{Ru}} + \mathcal{O}_{^{96}\mathrm{Ru}}}{\mathcal{O}_{^{96}\mathrm{Zr}} + \mathcal{O}_{^{96}\mathrm{Zr}}} \stackrel{?}{=} 1$

v_2 Ratio

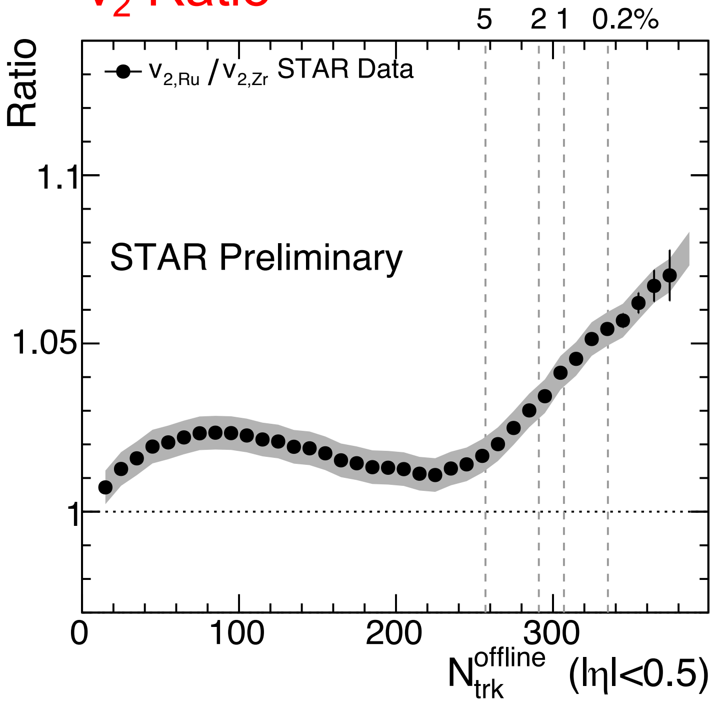

v_3 Ratio

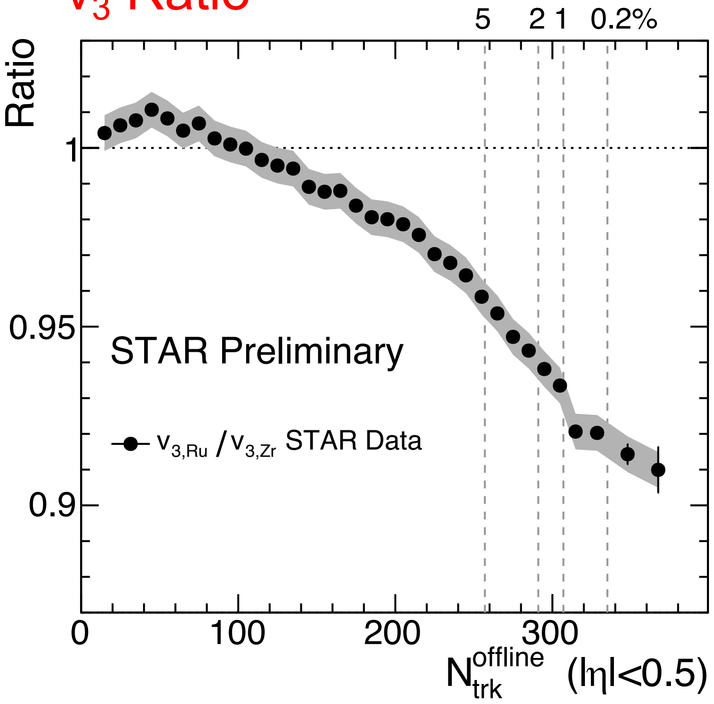

Nuclear structure via collectivity v_n ratio $\frac{\mathcal{O}_{^{96}\mathrm{Ru}}+\mathcal{O}_{^{96}\mathrm{Ru}}}{\mathcal{O}_{^{96}\mathrm{Zr}}+\mathcal{O}_{^{96}\mathrm{Zr}}} \stackrel{?}{=} 1$

v_2 Ratio

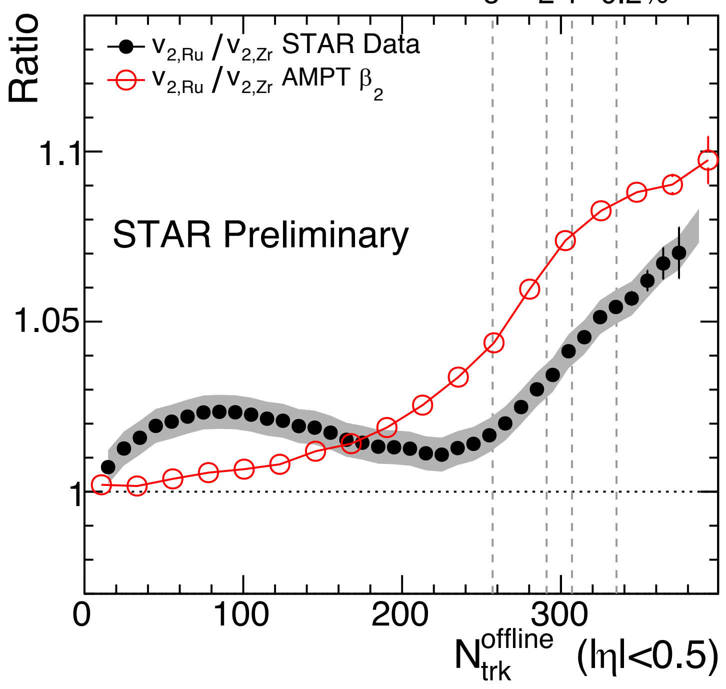

v_3 Ratio

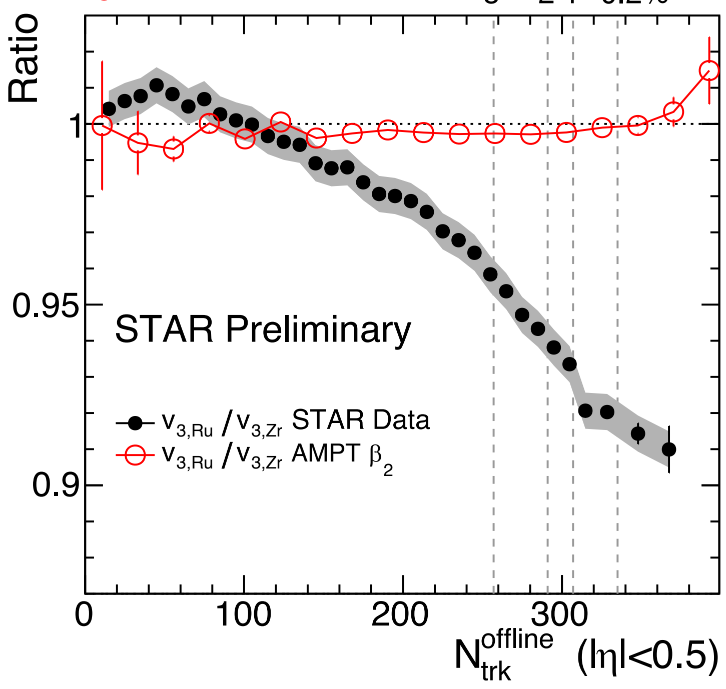

β_{2Ru} ~ 0.16 increase v_2, no influence on v_3 ratio

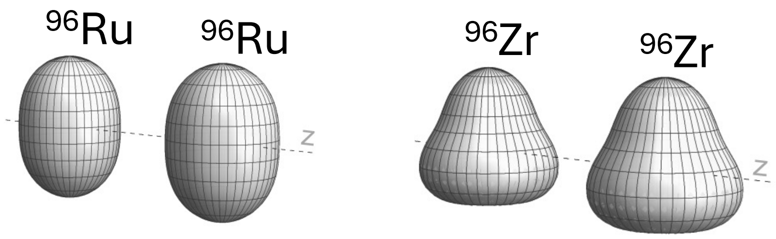

$\beta_{2,\mathrm{Ru}} = 0.16 \pm 0.02$

	$\Delta\beta_2^2$	$\Delta\beta_3^2$	Δa_0	ΔR_0
difference	0.0226	-0.04	-0.06 fm	0.07 fm

Current estimation is from transport model

C. Zhang and J. Jia, PRL128, 022301(2022); J. Jia, C. Zhang, PRC 107, L012901(2023)

Nuclear structure via collectivity v_n ratio $\frac{\mathcal{O}_{^{96}\mathrm{Ru}}+\mathcal{O}_{^{96}\mathrm{Ru}}}{\mathcal{O}_{^{96}\mathrm{Zr}}+\mathcal{O}_{^{96}\mathrm{Zr}}} \stackrel{?}{=} 1$

v_2 Ratio

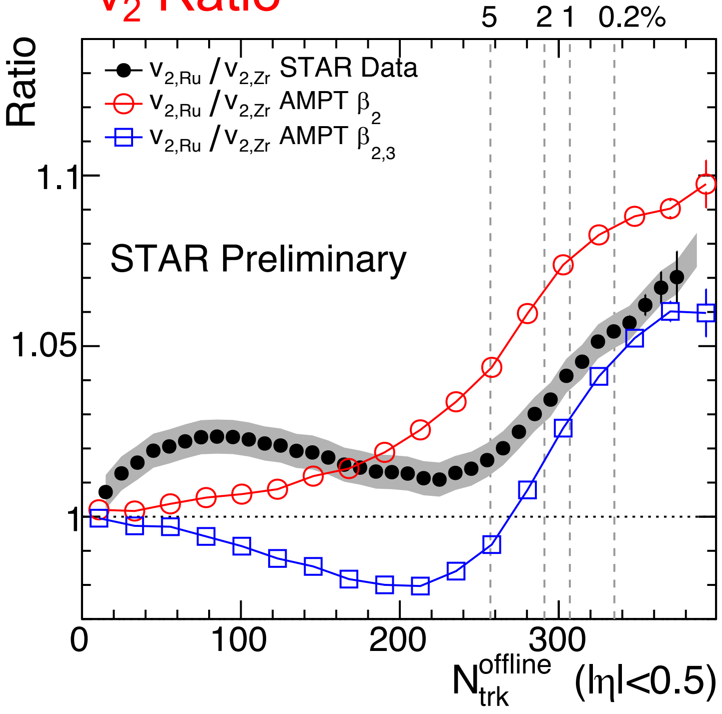

v_3 Ratio

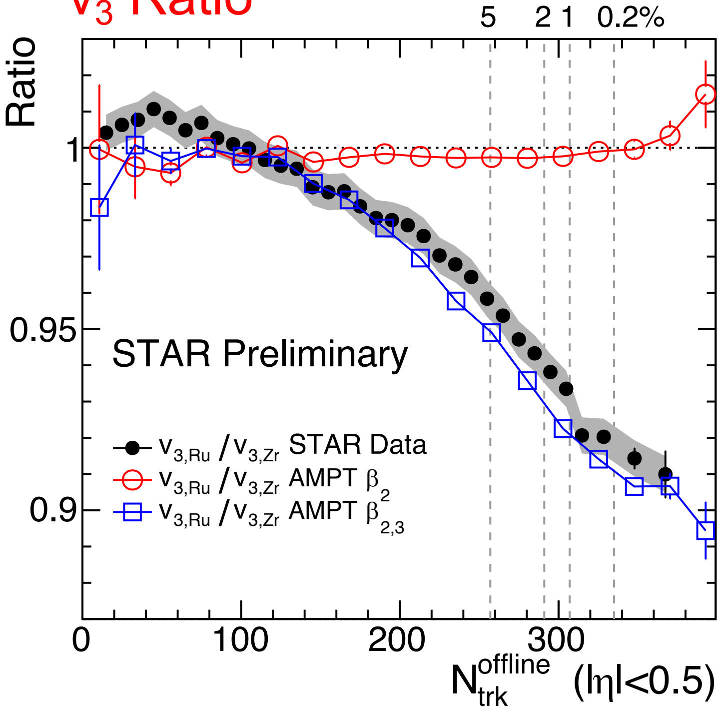

β_{2Ru} ~ 0.16 increase v_2, no influence on v_3 ratio

β_{3Zr} ~ 0.2 decrease v_2 in mid-central, decrease v_3 ratio

- Direct observation of octupole deformation in ^{96}Zr nucleus

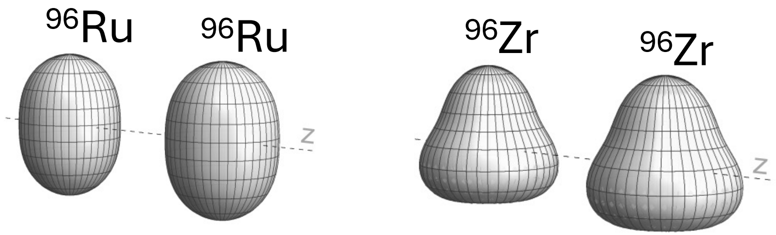

$\beta_{2,\mathrm{Ru}} = 0.16 \pm 0.02$ $\beta_{3,\mathrm{Zr}} = 0.20 \pm 0.02$

difference	$\Delta\beta_2^2$	$\Delta\beta_3^2$	Δa_0	ΔR_0
	0.0226	-0.04	-0.06 fm	0.07 fm

Current estimation is from transport model

C. Zhang and J. Jia, PRL128, 022301(2022); J. Jia, C. Zhang, PRC 107, L012901(2023)

Nuclear structure via collectivity v_n ratio $\frac{\mathcal{O}_{^{96}\mathrm{Ru}}+\mathcal{O}_{^{96}\mathrm{Ru}}}{\mathcal{O}_{^{96}\mathrm{Zr}}+\mathcal{O}_{^{96}\mathrm{Zr}}} \stackrel{?}{=} 1$

v_2 Ratio

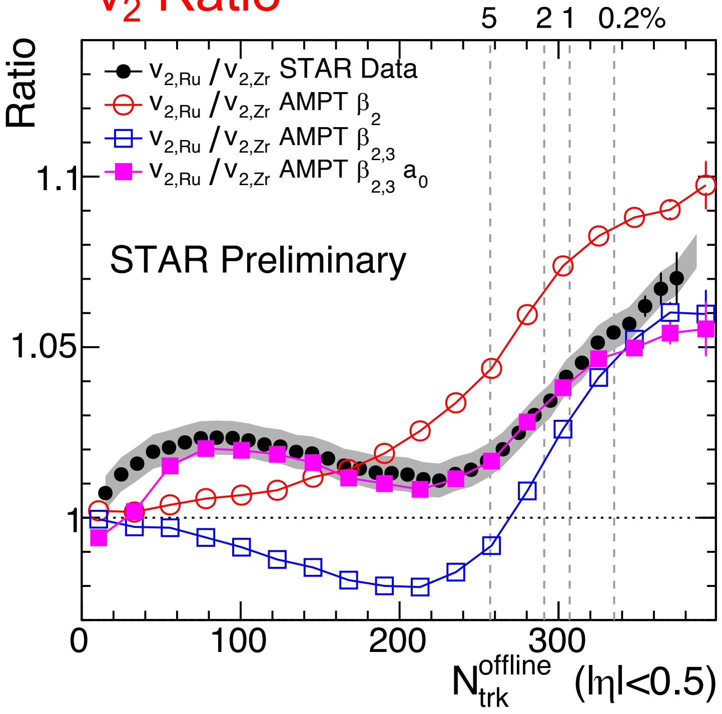

v_3 Ratio

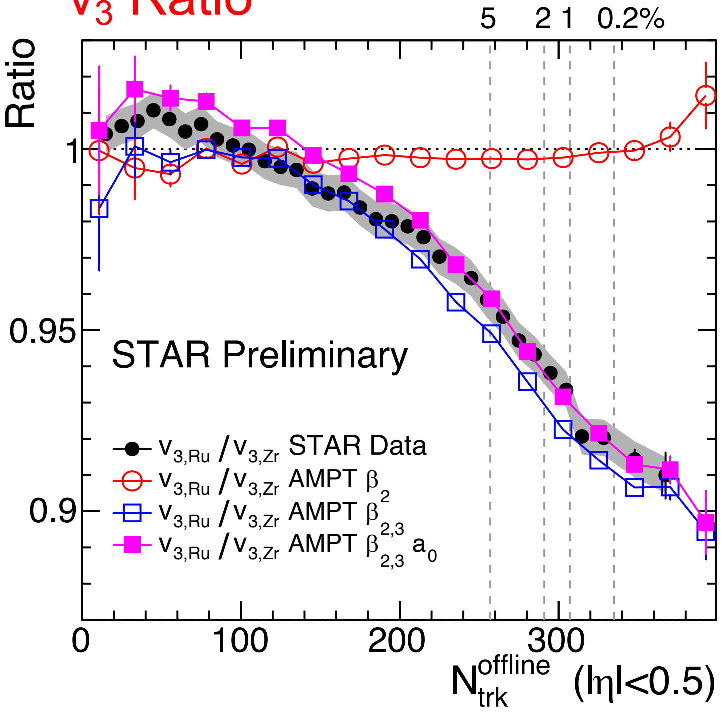

β_{2Ru} ~ 0.16 increase v_2, no influence on v_3 ratio

β_{3Zr} ~ 0.2 decrease v_2 in mid-central, decrease v_3 ratio

Δa_0 = -0.06 fm increase v_2 mid-central, small impact on v_3

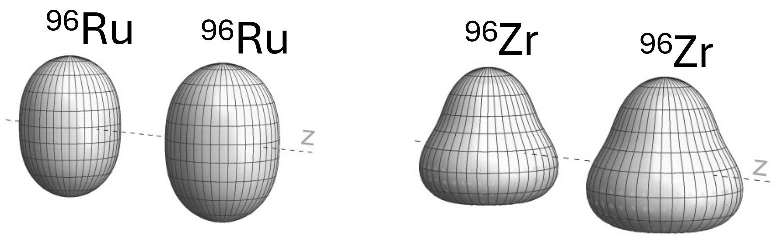

$\beta_{2,\mathrm{Ru}} = 0.16 \pm 0.02$ $\beta_{3,\mathrm{Zr}} = 0.20 \pm 0.02$

difference	$\Delta\beta_2^2$	$\Delta\beta_3^2$	Δa_0	ΔR_0
	0.0226	-0.04	-0.06 fm	0.07 fm

- Direct observation of octupole deformation in ^{96}Zr nucleus
- Imply the neutron skin difference between ^{96}Ru and ^{96}Zr

Current estimation is from transport model

C. Zhang and J. Jia, PRL128, 022301(2022); J. Jia, C. Zhang, PRC 107, L012901(2023)

Nuclear structure via collectivity v_n ratio $\frac{\mathcal{O}_{^{96}\mathrm{Ru}}+\mathcal{O}_{^{96}\mathrm{Ru}}}{\mathcal{O}_{^{96}\mathrm{Zr}}+\mathcal{O}_{^{96}\mathrm{Zr}}} \stackrel{?}{=} 1$

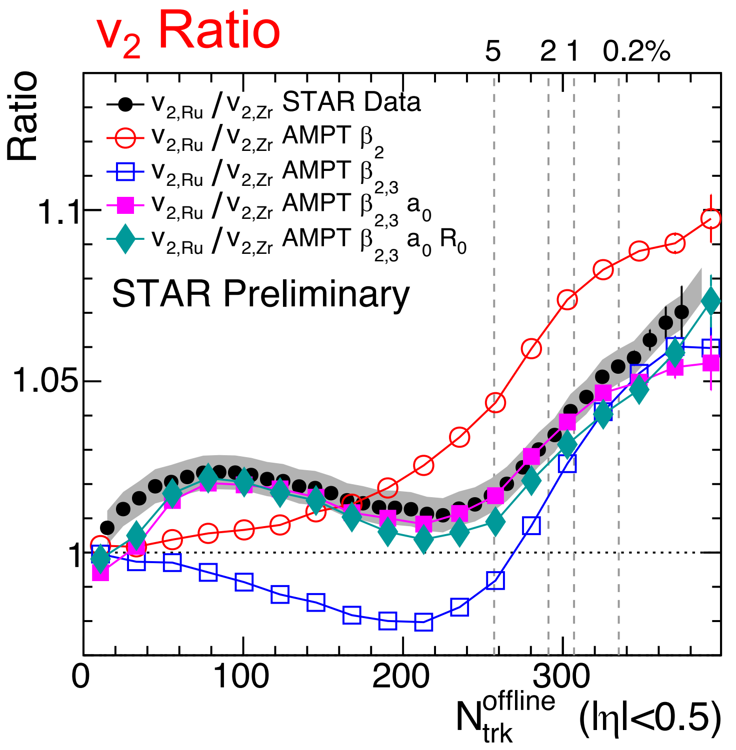

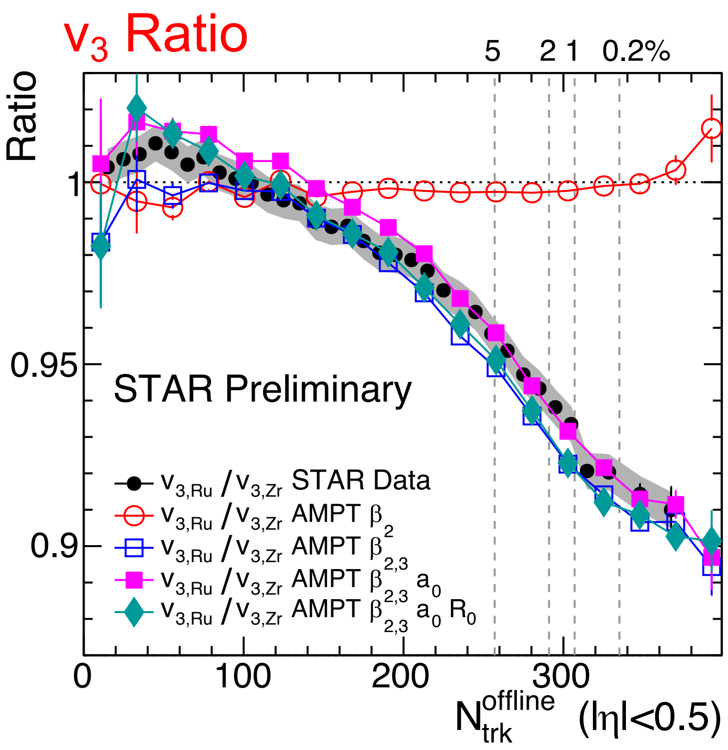

$\beta_{2Ru} \sim 0.16$ increase v_2, no influence on v_3 ratio

$\beta_{3Zr} \sim 0.2$ decrease v_2 in mid-central, decrease v_3 ratio

$\Delta a_0 = -0.06$ fm increase v_2 mid-central, small impact on v_3

Radius $\Delta R_0 = 0.07$ fm only slightly affects v_2 and v_3 ratio.

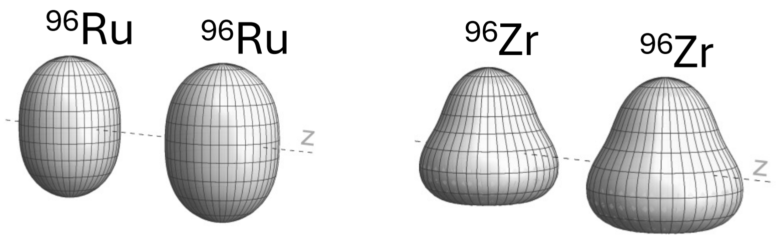

- Direct observation of octupole deformation in ^{96}Zr nucleus
- Imply the neutron skin difference between ^{96}Ru and ^{96}Zr
- Simultaneously constrain parameters using Bayesian analysis

$$R_{\mathcal{O}} \equiv \frac{\mathcal{O}_{\mathrm{Ru}}}{\mathcal{O}_{\mathrm{Zr}}} \approx 1 + c_1\Delta\beta_2^2 + c_2\Delta\beta_3^2 + c_3\Delta R_0 + c_4\Delta a$$

$\beta_{2,\mathrm{Ru}} = 0.16 \pm 0.02$ $\beta_{3,\mathrm{Zr}} = 0.20 \pm 0.02$

difference	$\Delta\beta_2^2$	$\Delta\beta_3^2$	Δa_0	ΔR_0
	0.0226	-0.04	-0.06 fm	0.07 fm

C. Zhang and J. Jia, PRL128, 022301(2022); J. Jia, C. Zhang, PRC 107, L012901(2023)

Current estimation is from transport model

Benchmarking tomography of many-body correlation in ^{16}O

from one-body distribution to many-body nucleon correlations

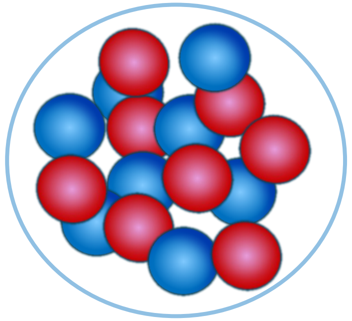

$$\rho(r) \propto \frac{1 + w\left(r^2/R^2\right)}{1 + e^{(r-R)/a_0}}$$

→ first-principle ab initio framework

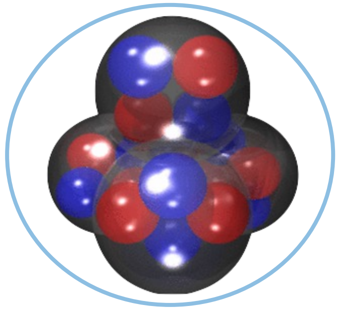

Hideki Yukawa 

“for his prediction of the existence of mesons
on the basis of theoretical work on nuclear forces”

Geometric tomography of ^{16}O nucleus

O+O run2021: 600M MB and 250M HM events

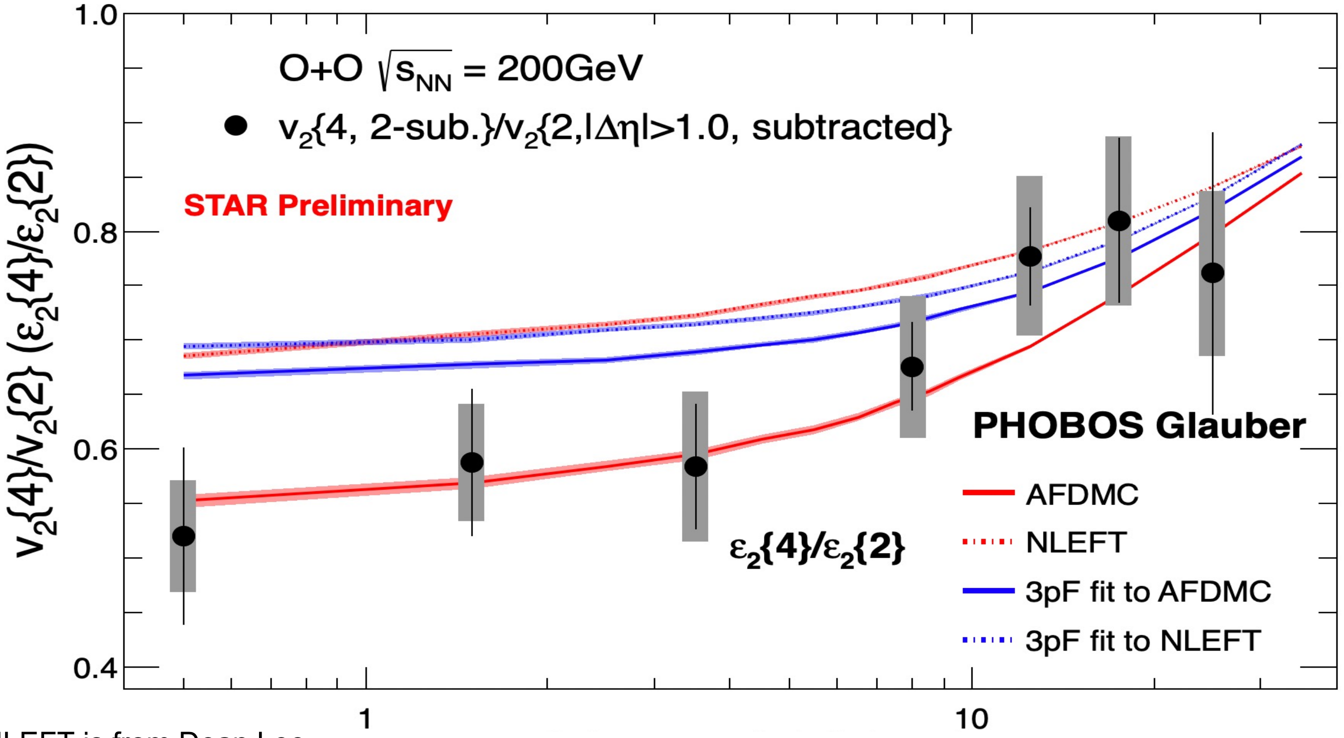

NLEFT is from Dean Lee.

$$(v_n\{2\})^2 = c_n\{2\} = \langle v_n^2 \rangle$$

$$(v_n\{4\})^4 = -c_n\{4\} = 2\langle v_n^2 \rangle^2 - \langle v_n^4 \rangle$$

$$\varepsilon_2\{2\}^2 = \langle \varepsilon_2^2 \rangle$$

$$\varepsilon_2\{4\}^4 = 2\langle \varepsilon_2^2 \rangle^2 - \langle \varepsilon_2^4 \rangle$$

$\varepsilon_2\{4\}$ /$\varepsilon_2\{2\}$ from three models:

1. WS is away from STAR data.

2. VMC and EFT have a visible difference.

Can many-nucleon correlations significantly impact the eccentricity fluctuations? YES!

VMC and EFT theory have visible differences describing the $v_2\{4\}/v_2\{2\}$. The interplay between sub-nucleon fluctuation and many-nucleon correlation.

STAR, PRL130, 242301(2023)

Geometric tomography of ^{16}O nucleus

O+O run2021: 600M MB and 250M HM events; dAu: 70M MB

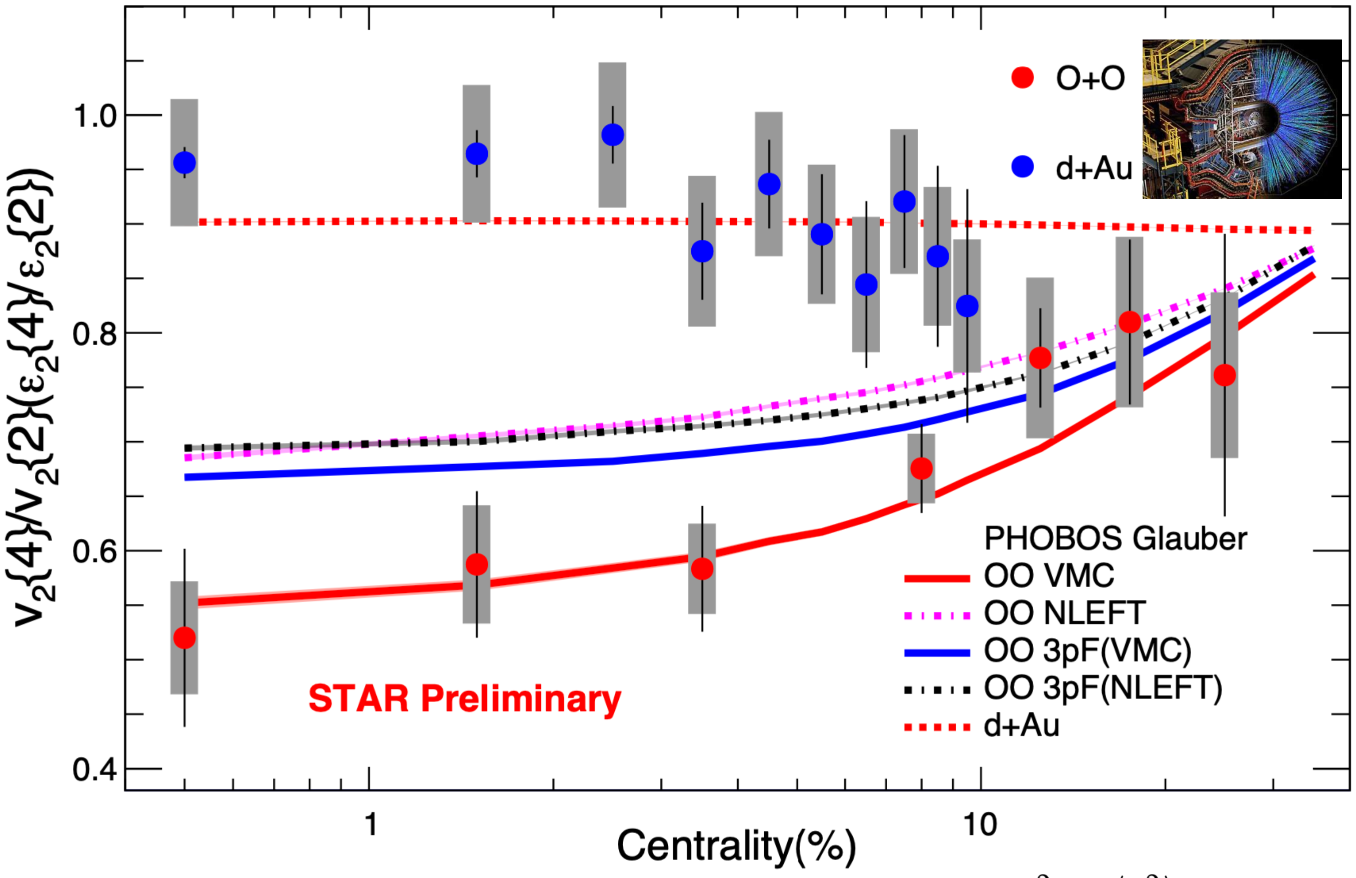

$$(v_n\{2\})^2 = c_n\{2\} = \langle v_n^2 \rangle$$
$$(v_n\{4\})^4 = -c_n\{4\} = 2\langle v_n^2 \rangle^2 - \langle v_n^4 \rangle$$

$$\varepsilon_2\{2\}^2 = \langle \varepsilon_2^2 \rangle$$
$$\varepsilon_2\{4\}^4 = 2\langle \varepsilon_2^2 \rangle^2 - \langle \varepsilon_2^4 \rangle$$

$\varepsilon_2\{4\}$ /$\varepsilon_2\{2\}$ from three models:

1. WS is away from STAR data.

2. VMC and EFT have a visible difference.

Can many-nucleon correlations significantly impact the eccentricity fluctuations? YES!

VMC and EFT theory have visible differences describing the $v_2\{4\}/v_2\{2\}$. The interplay between sub-nucleon fluctuation and many-nucleon correlation.

STAR, PRL130, 242301(2023)

Geometric scan elucidates nuclear tomography and **strong nuclear force?**

NLEFT is from Dean Lee; VMC is from PRC97, 044318 (2018)

more ab-initio/macroscopic model inputs are also needed.

Current O+O and d+Au at RHIC and p+O, O+O and Ne+Ne at LHC Run2025

C. Zhang, C. Chen, G. Giacalone, S. Huang, J. Jia, Y. Ma, PLB866, 139322 (2025)

Conclusions and Outlooks

1. **Intersection of nuclear structure and hot QCD across energy scales:**

→ better control variation of the QGP initial conditions

→ a novel way to unveil nuclear structure across energy scales

2. **The signatures of nuclear structure in nuclear collisions are ubiquitous:**

→ constrain β_2 and observe γ shape in ground-state ^{238}U: $\beta_{2\mathrm{U}} = 0.286 \pm 0.025$ $\gamma_U = 8.5^\circ \pm 4.8^\circ$

→ observe large β_3 in ^{96}Zr, a_0 difference between isobaric ^{96}Zr and ^{96}Ru

$\beta_{2,\mathrm{Ru}} = 0.16 \pm 0.02$ $\beta_{3,\mathrm{Zr}} = 0.20 \pm 0.02$

	$\Delta\beta_2^2$	$\Delta\beta_3^2$	Δa_0	ΔR_0
difference	0.0226	-0.04	-0.06 fm	0.07 fm

3. **Many potential applications from large to small heavy-ion collision systems :**

→ high-order β_3 and β_4 nuclear deformations (rigid/vibration)
→ rigid and soft γ (shape fluctuations/coexistence)
→ neutron skin
→ nuclear cluster in light nuclei (i.e.^{16}O and ^{20}Ne) at RHIC and the LHC
→ nucleosynthesis, nuclear fission, neutrinoless double-beta decay

Thank You

Activities for intersection of nuclear structure and high-energy nuclear collisions

Recently organized activities from 2022:

- RBRC workshop Jan 2022, link
- EMMI Taskforce May&Oct 2022, link
- ESNT workshop Sep 2022, link
- INT program Jan-Feb 2023, link
- Dalian workshop Aug 2023, link
- Beijing workshop April 2024, link
- CERN workshop Nov 2024, link

Intersection of nuclear structure and high-energy nuclear collisions:
2025 Program and Workshop, link

Continue the efforts to further constrain QGP initial conditions and nuclear structure across energy scales.

Some references for this article

nature › article metrics

Article metrics | Last updated: Sun, 25 May 2025 4:04:38 Z

https://www.nature.com/articles/s41586-024-08097-2

Imaging shapes of atomic nuclei in high-energy nuclear collisions

Access & Citations

53k Article Accesses	Data not available Web of Science	Data not available CrossRef

Citation counts are provided from Web of Science and CrossRef. The counts may vary by service, and are reliant on the availability of their data. Counts will update daily once available.

Online attention

- 41 tweeters
- 25 news outlets
- 4 Mendeley
- 3 blogs
- 2 Redditors
- 1 Facebook pages
- 1 Video uploaders

Altmetric calculates a score based on the online attention an article receives. Each coloured thread in the circle represents a different type of online attention. The number in the centre is the Altmetric score. Social media and mainstream news media are the main sources that calculate the score. Reference managers such as Mendeley are also tracked but do not contribute to the score. Older articles often score higher because they have had more time to get noticed. To account for this, Altmetric has included the context data for other articles of a similar age.

This article is in the 99th percentile (ranked 3,281st) of the 331,256 tracked articles of a similar age in all journals and the 77th percentile (ranked 268th) of the 1,198 tracked articles of a similar age in *Nature*

View more on Altmetric

Brookhaven National Laboratory Newsroom Media & Communications Office

Newsroom | Photos | Videos | Fact Sheets | Lab History | News Categories

https://www.bnl.gov/newsroom/news.php?a=122119

Contact: Karen McNulty Walsh, (631) 344-8350, or Peter Genzer, (631) 344-3174 share:

Imaging Nuclear Shapes by Smashing them to Smithereens

Scientists use high-energy heavy ion collisions as a new tool to reveal subtleties of nuclear structure with implications for many areas of physics

November 6, 2024

nature

Explore content | About the journal | Publish with us | Subscribe

nature › news & views › article

https://www.nature.com/articles/d41586-024-03466-3

NEWS AND VIEWS | 06 November 2024

Rare snapshots of a kiwi-shaped atomic nucleus

Smashing uranium-238 ions together proves to be a reliable way of imaging their nuclei. High-energy collision experiments reveal nuclear shapes that are strongly elongated and have no symmetry around their longest axis.

By Magda Zielińska & Paul E. Garrett

nature

Explore content | About the journal | Publish with us | Subscribe

nature › news › article

https://www.nature.com/articles/d41586-024-03633-6

NEWS | 06 November 2024

Smashing atomic nuclei together reveals their elusive shapes

A method to take snapshots of exploding nuclei could hold clues about the fundamental properties of gold, uranium and other elements.

By Elizabeth Gibney

nature

Explore content | About the journal | Publish with us | Subscribe

nature › nature podcast › article

https://www.nature.com/articles/d41586-024-03646-1

NATURE PODCAST | 06 November 2024

Surprise finding reveals mitochondrial ‘energy factories’ come in two different types

Mitochondria divide to share the load when nutrients are scarce – plus, how smashing atomic nuclei together helps identify their shapes.

By Benjamin Thompson & Emily Bates

Viscosity, nuclear parameters, and model variations

STAR, Nature 635, 67-72 (2024)
https://www.nature.com/articles/s41586-024-08097-2

1) Taking the ratios cancels the viscosity effects.

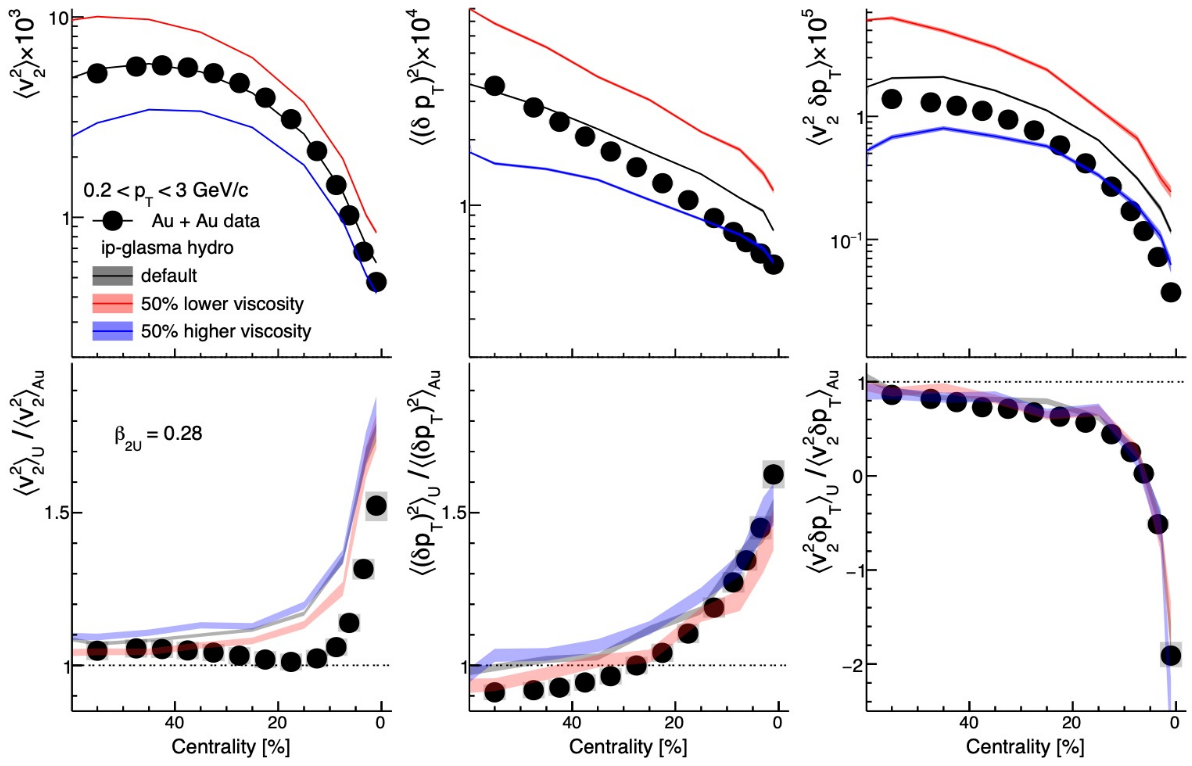

2) Effect from nuclear parameters are small, included as model systematics.

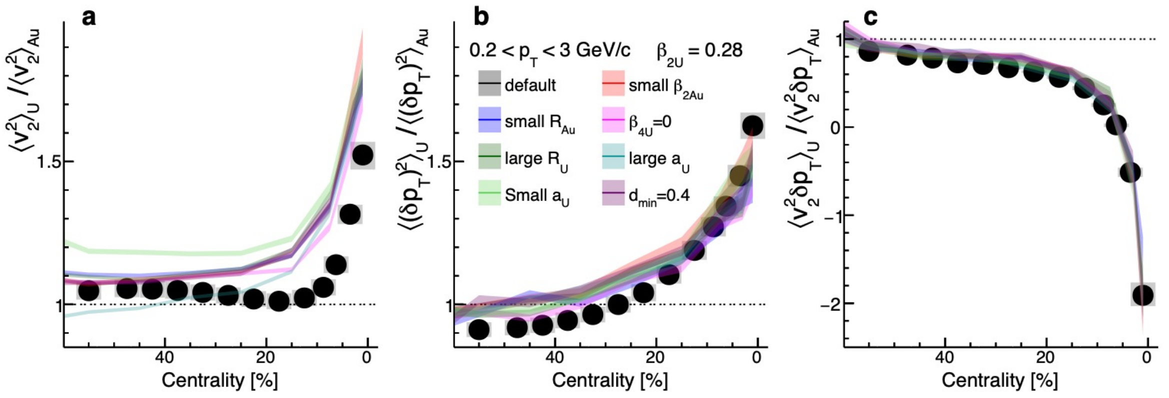

3) Another hydrodynamics model, Trajectum, shows rather consistent extractions even if it was not tuned to RHIC data.

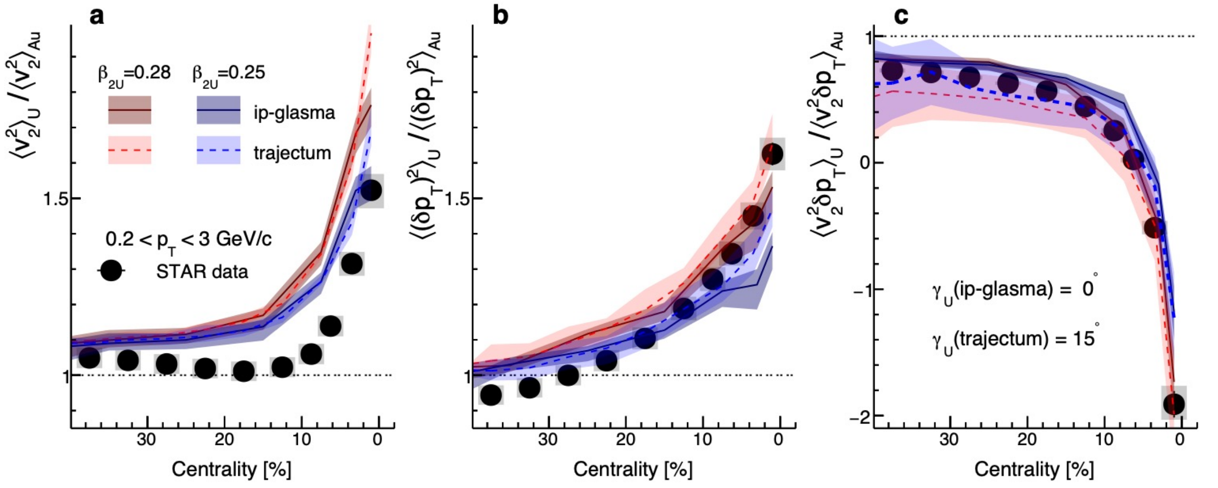

Extracted β_2 and γ values are robust.

Nuclear structure is inherent of heavy-ion probes

one-body distribution | two-body correlations | three-body correlations